Energy 328 (2025) 136621

Contents lists available at ScienceDirect

Energy

journal homepage: www.elsevier.com/locate/energy

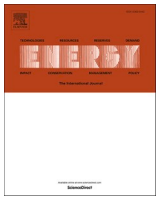

Experimental proof of a model-based real-time control of adsorption chillers

Valeria Palomba *, Antonino Bonanno, Giovanni Brunaccini, Fabio Costa, Davide La Rosa, Andrea Frazzica

National Research Council of Italy, Institute for Advanced Energy Technologies "Nicola Giordano", Salita S.Lucia Sopra Contesse 5, 98126, Messina, Italy

ARTICLE INFO

Handling Editor: Dr. Q. F. Ofelia Araujo

Keywords:
Dymola
Model predictive control
Sorption chillers

ABSTRACT

Adsorption chillers have been considered for waste heat utilization in both stationary and mobile applications, e. g. using waste heat from data centers and from internal combustion engines. Several efforts were made to improve the performance of such systems, mostly in terms of materials and components. However, a proper control strategy, adaptable to operating conditions that are continuously varying is paramount for the market development of adsorption chillers and heat pumps. The present work demonstrates the possibility of using a model-based control strategy that can be easily implemented in the standard PLCs of the chillers, without the need of expensive hardware. To this aim, an adsorption chiller prototype with nominal cooling power of 6 kW was tested and a simulation model was realized in Modelica/Dymola, which was then used for running several simulations and deriving an optimal "map of set-points". The beneficial effect of using the modified set-points for cycle time and flow rates was then proved experimentally by means of dedicated tests carried out with the optimal parameters. Results highlighted that there is always an improvement compared to the original conditions in the range of 6 %–31 % for the cooling power and, for the COP, is in the range 3 %–11 %.

NOMENCLATURE

A	Adsorption potential, kJ/kg
c_p	Specific heat, kJ/(kg K)
d_h	Hydraulic diameter, m
D	Diffusion coefficient, m^2/s
E	Characteristic energy of the working pair, kJ/kg
h	Specific enthalpy, kJ/kg
m	Mass, kg
$\dot{m}$	Mass flow, kg/s
n	Dubinin exponent, -
p	Pressure, Pa
$\dot{Q}$	Thermal Power, kW
R	Specific gas constant, kJ/(kg K)
S	Surface, m^2
t	Time, s
T	Temperature, °C
u	Specific internal energy, kJ/kg
U	Overall heat transfer coefficient, $W/(m^2 K)$
w	Uptake, kg/kg
w_0	Maximum uptake, kg/kg
Greek letters	
α	Heat transfer coefficient, $W/(m^2 K)$
β_v	Thermal expansion coefficient, 1/K
λ	Thermal conductivity, W/(m K)
ρ	Density, kg/m^3
Subscripts	
ads	adsorber
ev	evaporator
eq	equilibrium
in	inlet
out	outlet
sorb	adsorbent
Abbreviations	
AI	Artificial Intelligence
ANN	Artificial Neural Network
COP	Coefficient Of Performance
DA	Dubinin-Ashtakov
FMU	Functional Mock-Up Interface
HEX	Heat EXchanger
HTF	Heat Transfer Fluid
LDF	Linear Driving Force
ML	Machine Learning

(*continued on next column*)

(*continued*)

(*continued on next page*)

* Corresponding author.
E-mail address: valeria.palomba@cnr.it (V. Palomba).

https://doi.org/10.1016/j.energy.2025.136621
Received 7 March 2025; Received in revised form 9 April 2025; Accepted 15 May 2025
Available online 17 May 2025

(*continued*)

PLC	Programmable Logic Controller
SCP	Specific Cooling Power

1. Introduction

Adsorption chillers have been widely investigated and proposed for the use in various applications due to their ability to utilize waste heat and their environmentally friendly operation. Despite their advantages, controlling adsorption chillers poses significant challenges. The adsorption process is inherently complex, with a strong interdependence between operating temperatures and external settings (e.g. flow rates) on the sorption process itself, as discussed by some of the authors in Ref. [1]. Traditional control methods often struggle to maintain optimal performance due to the dynamic nature of these systems. This complexity calls for the development of advanced control strategies to ensure efficient and reliable operation.

The research on sorption chillers has been devoted, for several years, mostly to the development of new materials [2] and more efficient components [3–5], the importance of control to achieve an improvement in the performance of an adsorption chiller without extra expenses to the components has only been recognized in the last years [6]. In order to improve the performance of adsorption chillers and keep their output as stable as possible, one proposed solution is the re-allocation of cycle times by prolonging the adsorption time over desorption time. In order to achieve this result, some authors proposed the use of three-adsorbers' systems instead of the typical two-beds' ones [7,8]. The results proved that up to 20 % increase in cooling capacity can be achieved, but at the expenses of higher costs and complexity of the overall chiller. Finally, some authors recently proposed the use of fluidization technology also in adsorption chillers to improve heat and mass transfer [9,10], suggesting that significant benefits in both cooling and desalination applications could be achieved, but detailed efforts on components for mechanical fluidizations are still needed.

As a first approach to address the control challenges just by means of the definition of proper settings in a typical two-beds' configuration, researchers have explored the use of stochastic methods and various modeling approaches. Grey box models, which combine physical principles with empirical data, have been used to predict system behavior with reasonable accuracy. For instance, Albers [11] enhanced the characteristic equation method for single-stage absorption heat pumps by considering the realistic state of the solution entering the absorber and desorber (i.e. superheated or subccoled), achieving a 10 % improvement in system efficiency. Another approach widely used in the last years is the application of dynamic models, which capture the time-dependent behavior of the system and are based on the physical equations of the system. Bau and Bardow [12] demonstrated that a heat-flow-based control method based on a dynamic modelling of the adsorption chiller could achieve Pareto-optimal performance in one-bed adsorption chillers, resulting in a significant improvement in the coefficient of performance (COP) by up to 15 %. Gibelhaus et al. [6] implemented a dynamic model in Modelica/Dymola for integrated design and control strategies for full sorption chiller systems. This means that the model is intended to define both design parameters and control parameters. The methodology was applied to a selected case study (solar cooling), in which design parameters include the sizes of adsorption chiller, solar collector and cooling tower. The system control defines the volume flows of the circulating pumps, the air flow of the cooling tower and the cycle time. The results from the application of dynamic model proved that a 12 % energy efficiency could be achieved. However, the main drawback of this method is that it is not possible to run it in real-time, due to the computational expenses.

In more recent years, Artificial intelligence (AI) and machine learning (ML) techniques have shown great promise in enhancing the control of adsorption chillers. These techniques can analyze large datasets to identify patterns and optimize control strategies. For instance, neural networks and genetic algorithms have been used to improve the performance and efficiency of adsorption chillers. Krzywanski et al. [13] first proposed the optimization of a three-bed adsorption chiller using genetic algorithms and neural networks, resulting in a 10 % reduction in energy consumption. The same authors employed a model based on ML for the prediction of the effect of input parameters on an adsorption system for cooling and desalination, proving that the data-driven model can predict with high precision the effect of operating temperatures and flow rates [9,14]. Panahizadeh et al. [15] evaluated machine learning-based applications in forecasting the performance of single-effect absorption chiller networks, achieving a prediction accuracy of 95 %.Other authors employed Artificial Neural Networks (ANN) for the modelling and prediction of the performance of adsorption chillers. More in detail, the studies by Hong and Seong [16] and Kim et al. [17] have shown the effectiveness of ANN models in predicting energy consumption and optimizing adsorptions chiller and absorption chillers performance, respectively. Lazrak et al. [18] developed a model employing ANN for a single-effect absorption chillers and compared the results after training of the model with experimental data, achieving a deviation of 0.1–6.6 %. All these studies indicate, as possible outcome, the use of the ANN models for the implementation of a control strategy that improve the performance of an adsorption chiller, but no examples or guidelines on how to achieve this result are given.

On the other hand, it needs to be considered that the implementation of AI and ML techniques in industrial PLCs presents several challenges. The complexity of these algorithms often exceeds the computational capabilities of standard PLCs and requires the use of expensive solutions which can support cloud services [19], which is not always possible due to the installation in remote areas or where continuous internet connection is not accessible.

This article proposes a novel control method for adsorption chillers that addresses these challenges. The proposed method is designed to be simple to implement in industrial PLCs while maintaining high performance and efficiency. It is based on a validated dynamic model developed in Dymola/Modelica, that is used for the generation of high-quality synthetic data. The data are the processed using a meta-heuristic technique to define a complete map of settings according to the various operating conditions. The novelty of this approach lies in its simplicity and effectiveness, making it a valuable contribution to the field of adsorption chiller control.

2. Methodology

Fig. 1 presents the methodology followed for the present study: at first, a full characterization of the sorption chiller was carried out, using a dedicated testing equipment. The main aim of the experimental campaign was to measure the Specific Cooling Power (SCP) and the Coefficient of Performance (COP) of the prototype by considering both the external conditions and the possible settings for the system. The variable external conditions investigated include the temperature levels at which the chiller operates, whereas the variable settings applied include the speed of the pumps, and therefore the flow rates in all hydraulic circuits, and the cycle time.

Subsequently, a dynamic model for the chiller was realized in Modelica language using Dymola commercial software, which was validated using the data of tests under different conditions, to make sure the model was actually able to reproduce the behavior of the chiller reliably even when considering very different operating boundaries. The model was then exported as Functional Mock-Up Unit (FMU) and, using a dedicated Python script, several combinations of operating conditions and settings were evaluated.

Starting from the data collected, the most influential parameters were identified and used to fit the SCP and COP as a polynomial expression. The maximization of SCP and COP were then used as objective functions for a Mixed Integer Linear Programming Algorithm,

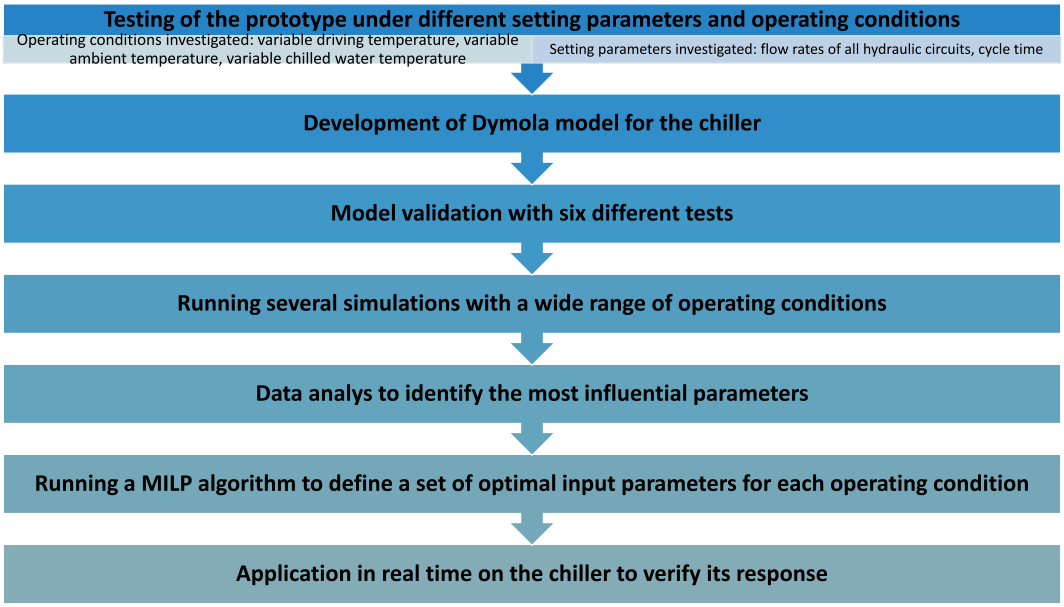

Fig. 1. Methodology of the study.

which gave as output a series of optimal settings for the different operating temperatures. The optimal settings were then tested on the prototype to calculate the gain in SCP and COP due to the use of the optimized logic.

3. Experimental

3.1. Prototype layout

Sorption chillers consists, in their "standard" layout, of two adsorbers, one evaporator and one condenser [20]. The adsorbers are usually vacuum chambers that contain a heat exchanger (HEX), where the sorbent is embedded or coated. The heat transfer fluid flowing in the HEX heats up/cools down the sorbent. In recent years, however, different layouts have been proposed, among which the concept of "process modules", employed for the prototype in this study. The process modules, schematically presented in Fig. 2, are part of the patented design of sorption chillers manufactured and patented by Fahrenheit GmbH [21].

A process module is made by an adsorption heat exchanger (AD-HEX), coated or glued with sorbent material and an evaporator/condenser heat exchanger (EC-HEX). The control valves (not visible in the figure), connect the process module to the hydraulic circuits to guarantee the proper operating temperature levels. During the adsorption phase the EC-HEX works as evaporator and is connected to the Low Temperature (LT) circuit, while the AD-HEX is connected to the medium temperature (MT) circuit. In this phase we have the useful effect because the refrigerant (water vapour) is absorbed by the sorbent material on the surface of AD-HEX. Due to the adsorption effect the pressure in the module decreases and the liquid water starts evaporating at the LT temperature (cooling effect). When the adsorbent material has reached the saturation condition all the water in the chamber has changed phase from liquid to vapour and has been adsorbed by AD-HEX. At this stage the adsorbent material needs to be regenerated, therefore the desorption phase starts. During the desorption phase, the AD-HEX is connected to the High Temperature (HT) circuit, while the EC-HEX works as condenser, therefore is connected to the MT circuit. In this phase the AD-HEX is heated and the refrigerant (water) is desorbed from the adsorbent material and is condensed by EC-HEX, now connected to the MT circuit.

Due to the fact that adsorption/desorption process is a discontinuous process, it is necessary to use two process modules for having a continuous cooling effect. Each process module contains an exact quantity of water, which is used as refrigerant during the evaporation/condensation phase as described above, corresponding to the maximum adsorption capacity of the adsorbent material employed.

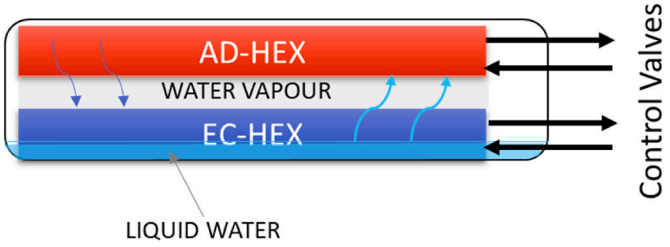

Fig. 2. Schematic view of process modules used in experimental tests.

3.2. Prototype development

The prototype used for the tests was manufactured by Fahrenheit GmbH and it was specifically designed for mobile applications, i.e. air conditioning on board of passengers' vessels. The main specifications of the prototype are given in Table 1. It is worth noticing that the prototype was designed so that the process modules are separated from the skid that contains the hydraulic valves and the electric cabinet. This choice was done because of the specific application meant for the vessel: in a real-scale system to be installed on board of a vessel, the passage for moving the complete assembly might not be sufficient and therefore splitting the process modules from the remaining components can facilitate transportation and installation. The overall process of development, that lead to the layout tested in the present work, can be found

Table 1
Main specifications of the prototype tested.

Parameter	Value
Working pair	Water/silica gel
Overall dimensions (adsorbers)	650 × 605 × 350 mm
Heat exchange area (adsorbers)	11 m^2
Heat exchange area (evaporator/condenser)	11 m^2
Sorbent mass	13 kg
Refrigerant mass	2 kg

elsewhere [22].

Some pictures of the prototype installed in the laboratory of CNR ITAE are visible in Fig. 3. It is possible to notice that the two process modules were installed syde by side. The prototype is also equipped with pumps for the three circuits and expansion vessels on the HT and MT circuits.

The hydraulic scheme for the prototype is shown in Fig. 4; the modules are connected in parallel and operate in counterphase, meaning that while one module is adsorbing/condensing, the other is desorbing/evaporating.

3.3. Experimental facilities

The testing rig used to experimentally characterize the prototype is described in detail in Ref. [22]. It consists of three water storage tanks that provide the High Temperature, Medium Temperature, and Low Temperature for the operation of the tested sorption chiller. The HT storage is a 1 m^3 storage with immersed resistances for a total heating power of 40 kW. It is also connected to a gas boiler with 60 kW heating capacity, thus accounting for a total of 100 kW heating capacity in the temperature range of 40–95 °C. The MT storage is a 1 m^3 storage connected to an air-to-water chiller with 50 kW thermal capacity and can be heated by an immersed electric heater of total 6 kW capacity; its operating range is 10 °C–50 °C. The LT storage is a 0.75 m^3 storage with a 30 % water/glycol mixture connected to a 13 kW air-to-water chiller and includes immersed electrical resistances, so that it can operate in the range of −7 °C to +40 °C. Temperature regulation on the three circuits of the system under test is accomplished using Siemens high-speed valves mixing between the inlet and exit from the storage tank. Plate heat exchangers are used to achieve hydraulic separation between the testing rig and the system under test. The P&ID of the testing rig is shown in Fig. 5.

The list of sensors used is reported in Table 2.

3.4. Testing procedure and conditions

The testing procedure followed is intended to guarantee that stable conditions are achieved and that the tests are carried out in a reproducible way. It consists of the following stages.

a. The experimental test session begins with the conditioning of the thermal storage systems in the testing rig. This is done by setting the desired temperature on the LabVIEW software used to control the testing rig.
b. After the storage systems of each of the three circuits have reached the predefined temperatures, the set-point temperature for the inlet temperature of all circuits is set on the LabView software.
c. The modbus command for starting the chiller is given through LabView and the test is then started.
d. The process module takes approximately 5 cycles to reach a steady state operating condition. This is set as the duration of the test.
e. After 5 cycles, the chiller is stopped.

Tests were carried out changing the operating temperatures (HT inlet, MT inlet and LT inlet), as well as the flow rates in the various circuits and the cycle time. The operating conditions tested are listed in Table 3.

The main parameters evaluated during the tests were the thermal powers, the cooling energy and the COP.

The thermal power of each hydraulic circuit was calculated as:

$$\dot{Q} = \dot{m}\, c_p\, (T_{in} - T_{out}) \quad (1)$$

Where $\dot{Q}$ [kW] is the thermal power, $\dot{m}$ is the mass flow rate [kg/s] of the heat transfer fluid, cp [kJ/(kg K)] is the specific heat and T [°C] is the temperature of the heat transfer fluid.

In addition, the overall energy at the evaporator, which represents the useful effect for the application, was calculated as:

$$Q_{ev} = \int \dot{m}\, c_p\, (T_{in} - T_{out})\, dt \quad (2)$$

The COP was calculated as the ratio of the useful effect over the thermal energy supplied to drive the process.

$$COP = \frac{Q_{ev}}{Q_{HT}} = \frac{\int \dot{m}_{LT}\, c_p\, (T_{in} - T_{out})_{LT} dt}{\int \dot{m}_{HT}\, c_p\, (T_{in} - T_{out})_{HT} dt} \quad (3)$$

The integral heat at the HT and LT circuits were calculated over the entire test time.

3.5. Results

3.5.1. Typical trends

Figs. 6 and 7 present the typical trends recorded during a test with HTin: 75 °C, MTin: 28 °C and LTin: 16 °C, 1200 s cycle time and nominal flow rates in the three circuits, as given by the manufacturer of the chiller. The trends are those typical of a sorption chiller, with cyclic behavior. The temperatures in the HT circuit increase quickly at the beginning of each phase as desorption process proceeds, and at the same time the LT temperatures decreases immediately as adsorption starts and then increases slightly due to the reduced driving force of the process. The MT process increases extremely rapidly due to the need of dissipating the adsorption heat and the condensation heat, as well as the sensible heat for cooling down the process module that was undergoing desorption in the previous half cycle.

The power trends follow the temperature trends. HT and LT temperatures are presented as positive powers, since they are adsorbed by the system, whereas released power (MT) is indicated as negative It is worth noticing that, despite the typical discontinuous behavior of the sorption chiller, the cooling effect (purple line) is quite constant, with the exception of approximately 30 s during the change of each phase, corresponding to the isosteric heating/cooling of the adsorber. This result is extremely important, since it demonstrates the possibility of guaranteeing a continuous service to the rooms/devices that are being cooled down by the chiller.

3.5.2. Performance data – typical operating conditions

The first part of the testing campaign was dedicated to the verification of performance under typical operating conditions, considering low-temperature waste heat (T < 80 °C) and mild to warm ambient conditions.

The cooling power measured is shown in Fig. 8, as a function of the temperature lift MT-LT, which is defined as.

$$(MT - LT) = MT_{in} - LT_{out} \quad (4)$$

The experimental points are distributed in different groups, according to the regeneration (HT) temperature. As it is expected, higher regeneration temperatures lead to higher cooling power. For each regeneration temperature set, the points follow a quadratic trend, with decreasing cooling power when the temperature lift increases, which is a typical behaviour for adsorption chillers widely reported in the scientific literature. It is however interesting to notice that the points at 75 °C and 77 °C are almost superimposed, which is justified by the small temperature difference between the two sets. Interestingly, also the points at 62 °C and 72 °C show similar values, which is however due to the fact that the tests at 62 °C are done with a higher evaporation temperature compared to those at 72 °C.

The second parameter analyzed is the coefficient of performance (COP). The corresponding results, derived from the same experimental tests as for cooling power, are illustrated in Fig. 9. Compared to the cooling capacity, the COP exhibits an inverse trend, with higher values observed at lower heat source temperatures. This behavior, commonly

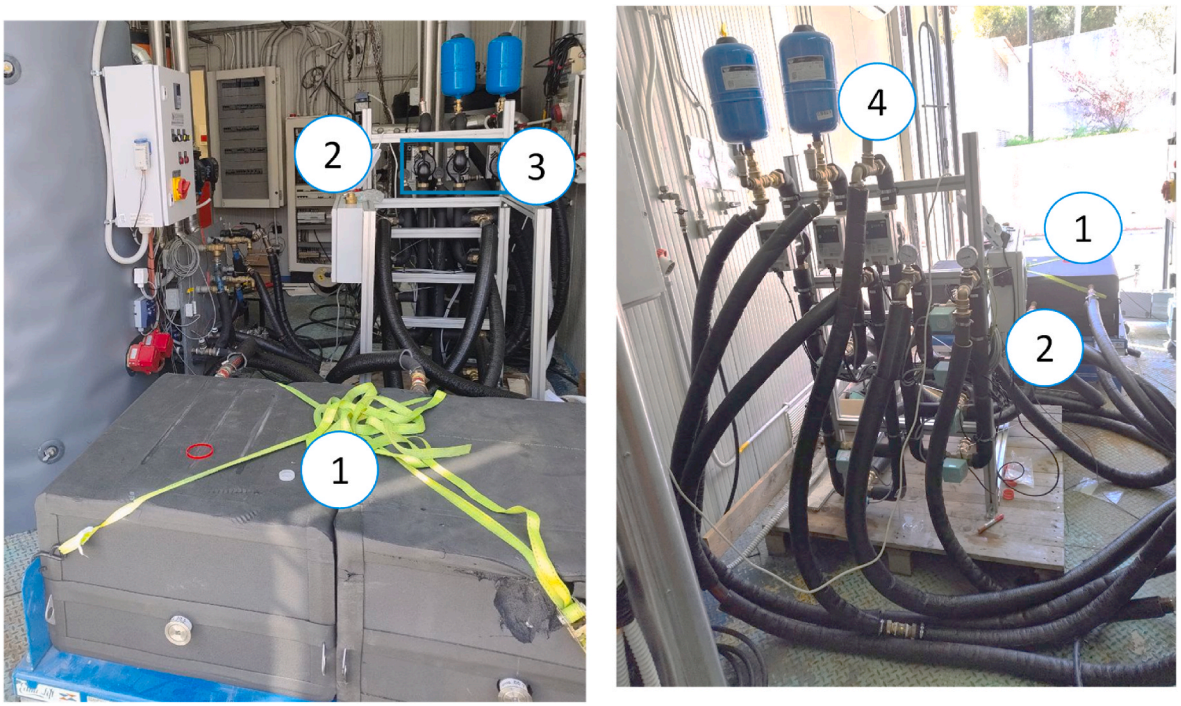

Fig. 3. Prototype installed in the lab of CNR ITAE. 1: process modules. 2: electric cabinet. 3: pumps. 4: hydraulic group with valves and expansion vessels.

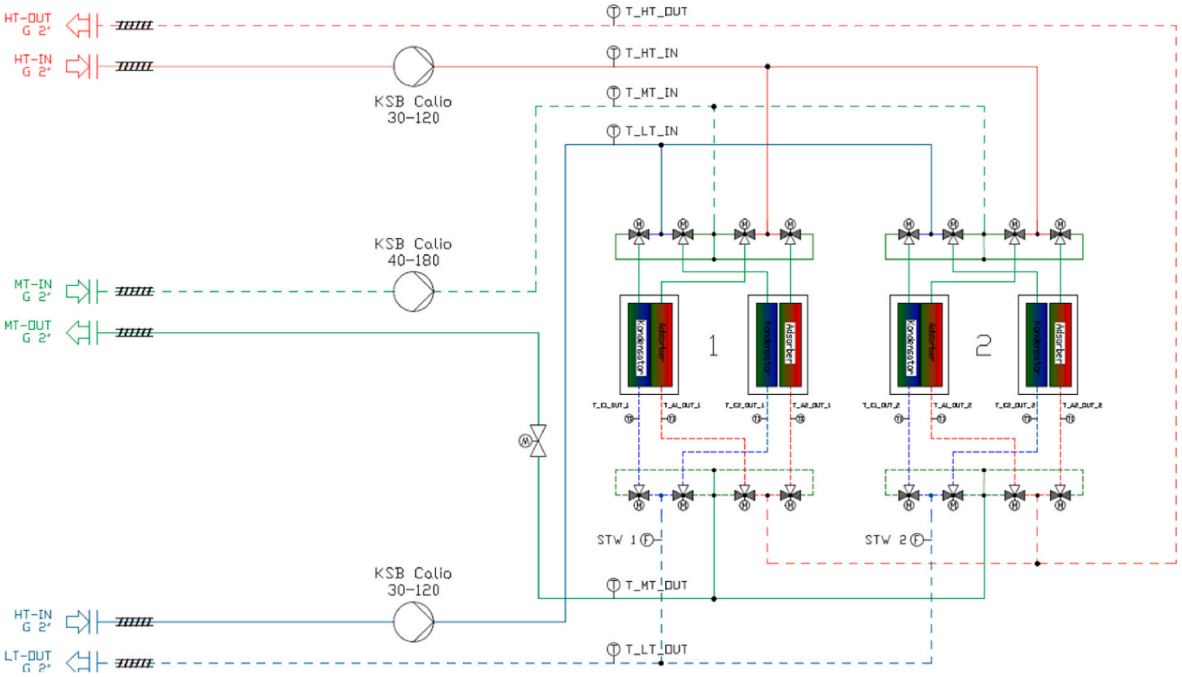

Fig. 4. Hydraulic scheme of the prototype.

documented in the literature, can be attributed to reduced heat losses during desorption at lower temperatures. In general, the COP decreases as the temperature lift increases.

However, as shown in Fig. 9, variations in other operational parameters, such as cycle time—automatically regulated during these experiments using Fahrenheit's standard calculation algorithm—and flow rates within the various circuits, significantly influence the COP. Notably, the achieved COP values remain relatively high, exceeding 0.5 under several conditions. This performance can be partly attributed to the compact design of the chiller, which incorporates shorter hydraulic circuits, smaller and faster valves, and other efficiency-enhancing features. Moreover, the achieved COP values are competitive, even compared to prototype systems reported in the literature, highlighting the effectiveness of the construction approach employed in this study.

3.5.3. *Performance data – sensitivity analysis on settings*

The second phase of the testing campaign aimed to investigate the influence of key operating parameters on the delivered cooling power and COP. The parameters examined included cycle time and heat transfer fluid flow rates across the various circuits. The outcomes are

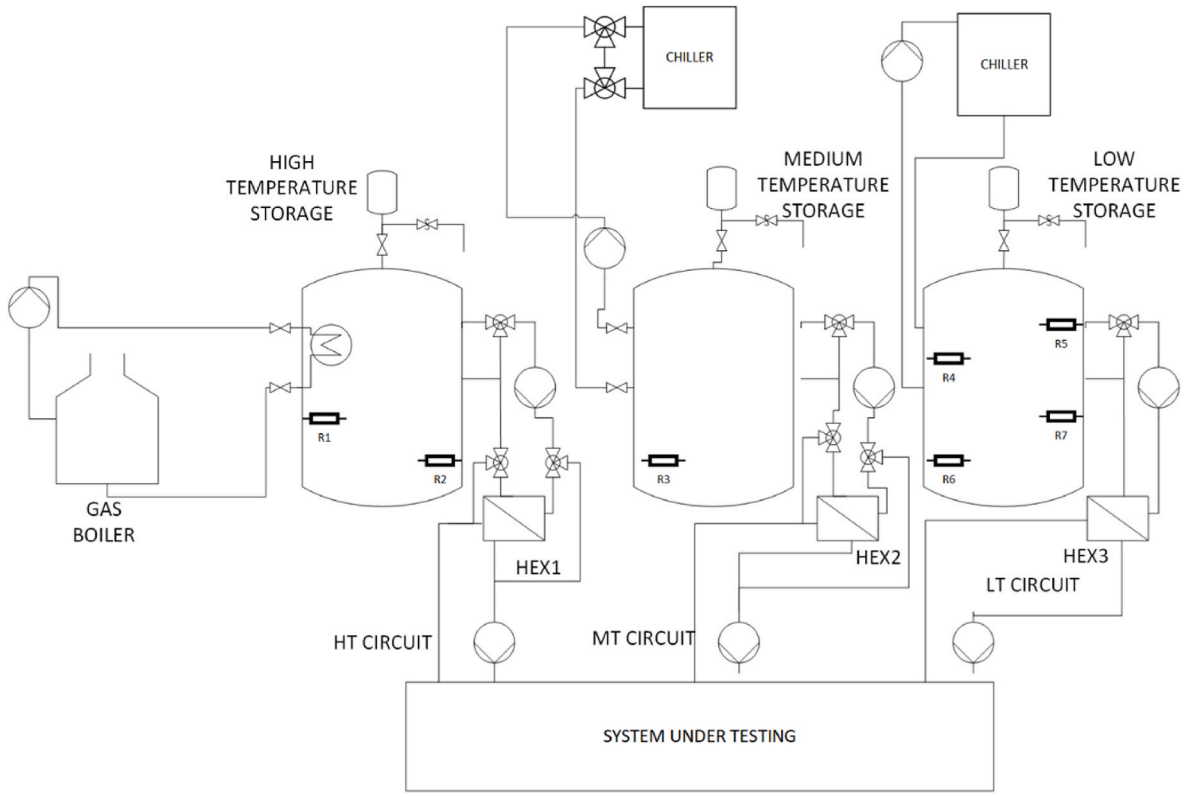

Fig. 5. P&ID of the testing rig.

Table 2
List of sensors used during testing.

Sensor	Accuracy	Measured parameter	Installation location
Type T thermocouples	Class A	Inlet and outlet temperature of all hydraulic circuits.	Testing rig
Magnetic flow meters MagView MVM-100-Q	±1 % RD	Flow rates in all hydraulic circuits.	Testing rig
Pt1000	Class A	Inlet and outlet temperatures of the hydraulic circuits of the adsorption chiller	Process module under testing
CB-1000 electricity meter	±0,2 % FS	Electricity consumption	Testing rig

presented in Fig. 10. Cycle times are expressed as intervals, as the programmable logic controller (PLC) of the chiller defined an allowable range during this testing phase. Within this interval, the chiller's internal software autonomously managed the cycle time.

Under the tested conditions, cooling power was observed to decrease with longer cycle times, while the COP increased. This behavior is typical for adsorption systems: as cycle time increases, the average cooling power diminishes because a greater portion of the cycle delivers lower cooling power, reducing the mean output. Conversely, COP—calculated on an energy basis—rises with longer cycle times, as the extended duration facilitates greater energy release.

For the specific conditions tested (70 °C HT inlet, 26 °C MT inlet, 16 °C LT inlet, and flow rates of 0.9 kg/s for HT, 1.2 kg/s for MT, and 1.0 kg/s for LT, closely matching the nominal values recommended by Fahrenheit), cooling power ranged from 4.8 kW to 4.3 kW, while COP values remained relatively high, between 0.53 and 0.65.

Fig. 11 depicts the impact of flow rates under the same temperature conditions (70 °C HT, 26 °C MT, 16 °C LT) with a fixed cycle time of 1000 s. Fig. 11a shows the influence of HT flow rate, which has a minimal effect on COP, with values ranging from 0.52 to 0.55, slightly higher at increased HT flow rates. In contrast, cooling power increased with higher HT flow rates, rising from 6.5 kW at 0.46 kg/s to 6.7 kW at 0.91 kg/s, consistent with observations for larger prototypes.

The effect of MT flow rate, the largest due to the need to dissipate both adsorption and condensation heat to the environment, was evaluated using five different values (Fig. 11b). The COP exhibited a minor decline, from 0.57 at 0.83 kg/s to 0.52 at 1.67 kg/s. Cooling power displayed a parabolic trend: increasing MT flow rate boosted cooling power, but at lower flow rates (0.83 kg/s), cooling power was approximately 15 % lower (6.0 kW) than at the highest flow rate tested (1.67 kg/s), where it reached 6.7 kW.

Fig. 11c illustrates the impact of LT flow rate. The COP increased significantly from 0.45 to 0.60 as the flow rate rose from 0.25 kg/s to 0.85 kg/s, followed by a reduction to 0.54 at 1.03 kg/s. Cooling power also showed a marked increase from 4.2 kW to 5.8 kW when the flow rate rose from 0.25 kg/s to 0.85 kg/s but remained nearly constant beyond 0.85 kg/s.

Table 3
Testing conditions.

HT IN	MT IN	LT IN	HT FLOW	MT FLOW	LT FLOW	cycle time
65 °C, 70 °C, 75 °C	25 °C, 27 °C 30 °C, 32 °C, 35 °C	12 °C, 16 °C, 18 °C, 20 °C	nominal, 25 % of nominal, 50 % of nominal, 120 % of nominal	nominal, 25 % of nominal, 50 % of nominal, 120 % of nominal	nominal, 25 % of nominal, 50 % of nominal, 120 % of nominal	600 s, 800 s, 1000 s, 1200 s

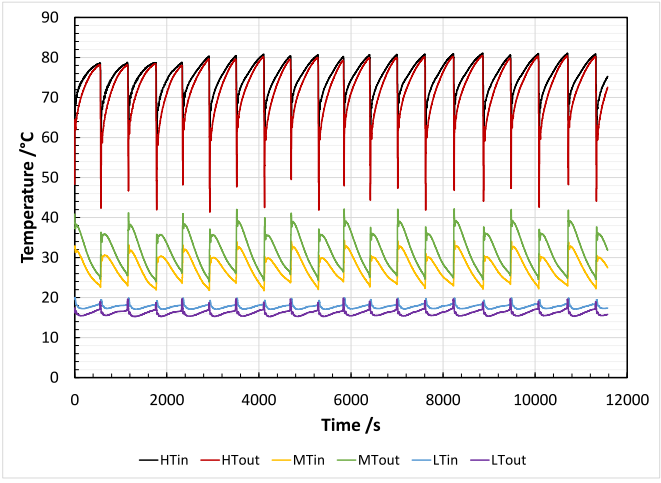

Fig. 6. Typical trends of temperatures during a test with the prototype.

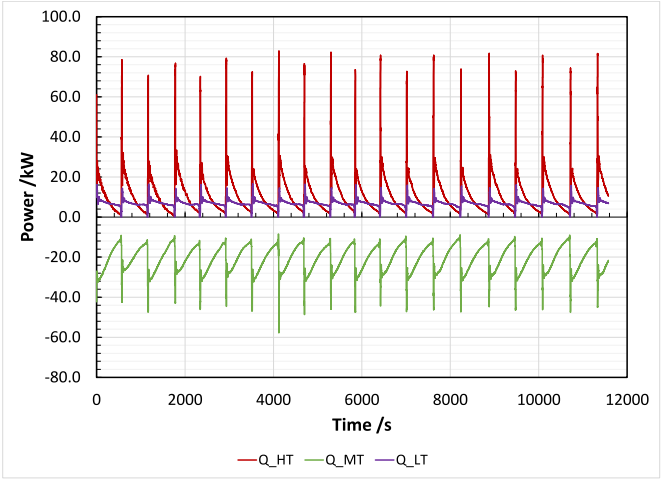

Fig. 7. Typical trends of thermal powers during a test with the prototype.

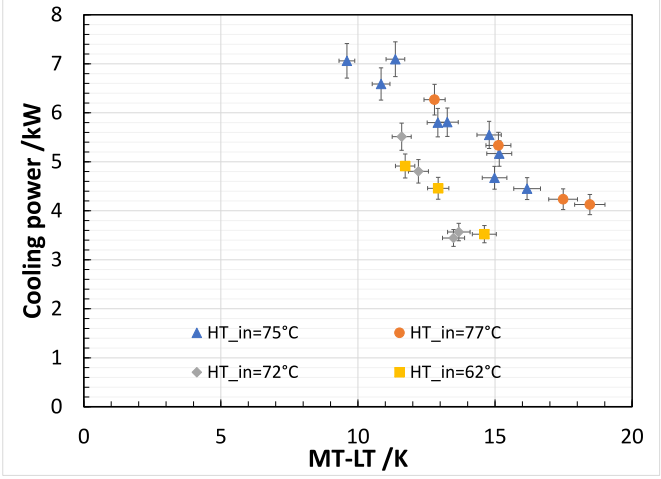

Fig. 8. Cooling power as a function of the temperature lift - prototype for control logic development.

These findings highlight the complex interdependencies between operating parameters, emphasizing the need for a systematic, model-assisted approach to define optimal system settings. This topic will be explored in detail in section 5.

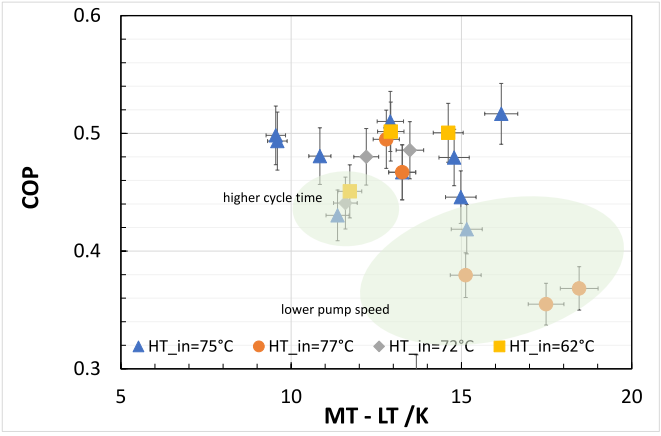

Fig. 9. COP as a function of the temperature lift - prototype for control logic development.

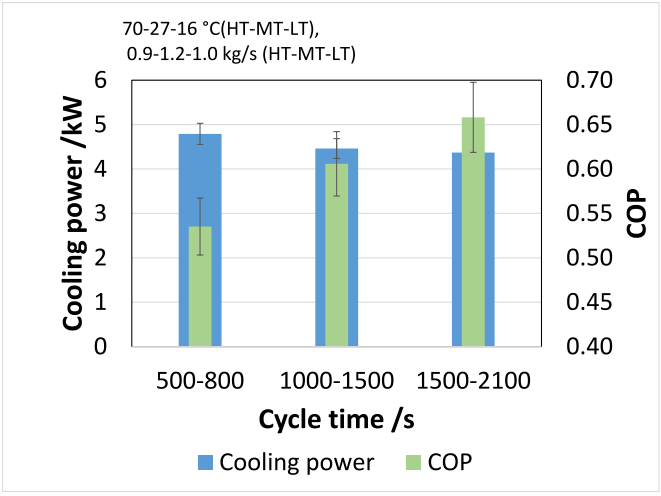

Fig. 10. Cooling power and COP for different cycle times.

4. Numerical

4.1. Model highlights and main equations

The implemented dynamic model is built upon the SorpLib library, which consists of components for sorption processes modeled using the Modelica language and developed by the Institute of Technical Thermodynamics at RWTH Aachen University.[1] Building upon this foundation, CNR has developed a library of calibrated components, which is based on experimental research on the sorption dynamics of various configurations and is discussed in details in Ref. [21]. Here, the main assumptions and equations of the model are presented.

The model realized is a dynamic model based on heat and mass transfer equations for all the components in the sorption chiller. It is worth noticing it uses a lumped approach, so only a discretization in the heat transfer fluid path of the heat exchangers is considered, all the other components are treated as single nodes. A picture of the model for a process module with the layout presented in this paper is shown in Fig. 12. The main components of the process module are.

[1] https://git.rwth-aachen.de/ltt/SorpLib.

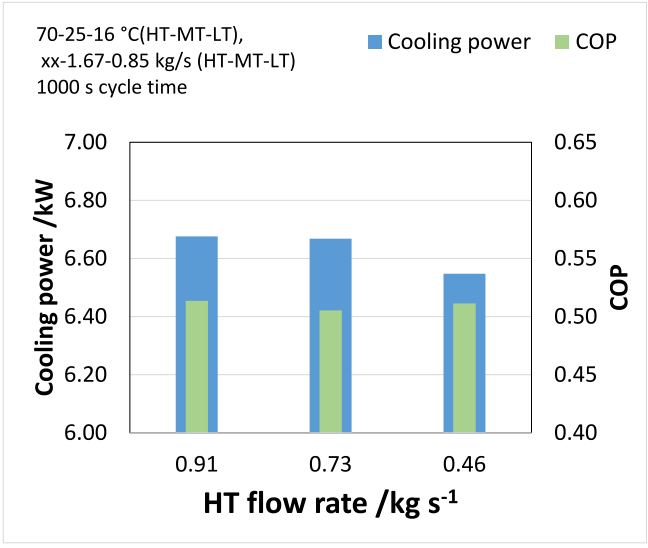

(b)

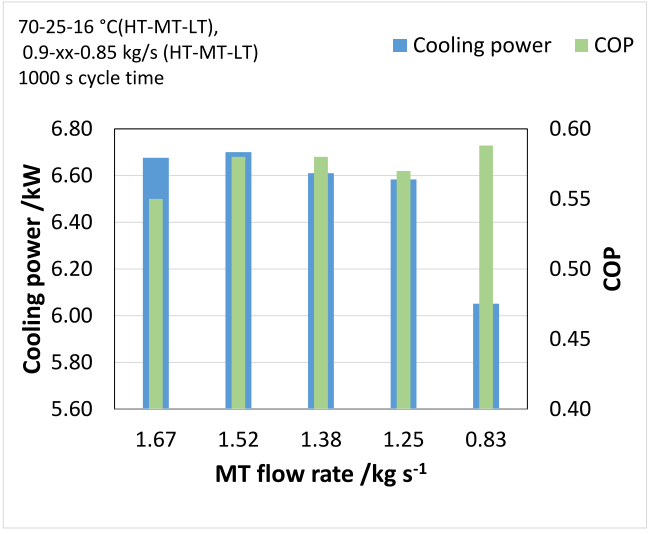

(c)

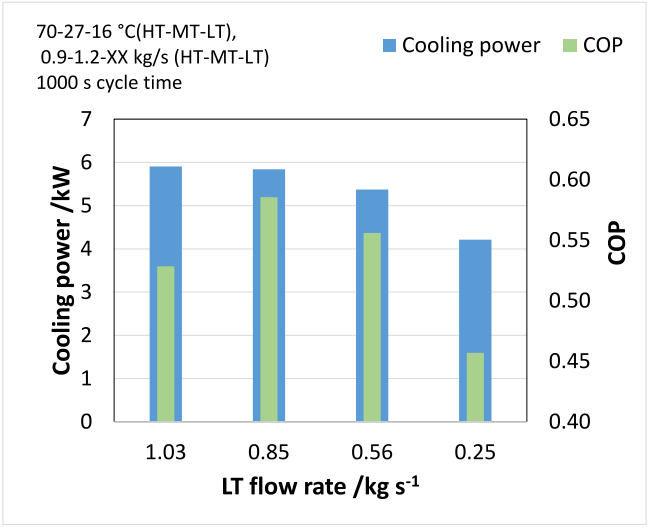

Fig. 11. Cooling power and COP for different flow rates. (a) Variation of HT flow rate; (b) variation of MT flow rate; (c) variation of LT flow rate.

- The model for the equilibrium of the sorbent, that allows calculating the uptake of refrigerant as a function of temperature and pressure;
- The models for the mass transfer, i.e. refrigerant vapour transport from the adsorber to the evaporator/condenser;
- The heat and mass balance equations for the adsorber and the evaporator/condenser;
- The model for the vapour/liquid equilibrium of the refrigerant;
- The models for the heat exchangers of the adsorber and the evaporator/condenser.

The adsorption equilibrium is described using the Dubinin-Astakhov (D-A) equation [23], as follows:

$$X_{eq} = X_0 \exp\left[-\left(\frac{A}{E}\right)^n\right], \quad 5$$

The parameters for the D-A equation are obtained by fitting the isotherms data measured at CNR and presented in Ref. [24].

In addition, the model for the adsorber includes the equations for heat and mass transfer. Heat balance of the adsorber is given by:

$$\frac{dU_{sorb}}{dt} = u_w \cdot \frac{d(M_w)}{dt} + \left(M_w c_{p,w} + M_{sorb} \cdot c_{p,sorb}\right) \cdot \frac{dT_{sorb}}{dt} = \dot{M}_{w,in} h_{in} - \dot{M}_{w,out} h_{out} + \dot{Q}_{sorb,htf} \quad 6$$

Where U is the internal energy [J], u is the specific internal energy [J/kg], M is the mass [kg], cp is the specific heat [J/(kg K)], T is the temperature [K], h is the specific enthalpy [J/kg] and $\dot{Q}_{sorb,htf}$ [W] is a term indicating the heat transfer between the heat transfer fluid and the sorbent. The subscripts "w" refers to water, whereas "sorb" to the sorbent material.

The heat exchanged with the heat transfer fluid is given by:

$$\dot{Q}_{sorb,htf} = (UA)_{HEX} \cdot \left(T_{htf} - T_{sorb}\right) \quad 7$$

where $(UA)_{HEX}$ is the overall heat conductance between metal and adsorbent.

The mass balance equation is:

$$\frac{dM_w}{dt} = \dot{M}_{w,in} - \dot{M}_{w,out} \quad 8$$

The variation of the adsorption uptake as a function of time is described by means of the linear driving force (LDF) approach, which is expressed as:

$$\frac{dX}{dt} = \frac{1}{M_{sorb}} \cdot \frac{dM_w}{dt} = k_{LDF} \cdot \left(X_{eqi}(p,T) - X\right) \quad 9$$

Where X is the uptake [kg/kg], X_{eqi} refers to the uptake at equilibrium under the current pressure and temperature conditions and k_{LDF} is the diffusion coefficient. This coefficient is used as a calibration parameter and is calculated from experimental data.

The evaporator/condenser model developed is based on the implementation already described in Ref. [21] and includes the heat and mass transfer equations for the refrigerant which is in vapour/liquid equilibrium conditions. The equations for heat and mass transfer are:

$$\frac{dm}{dt} = \dot{m}_v + \dot{m}_l \quad 10$$

$$\frac{dU}{dt} = \dot{H}_v + \dot{H}_l + \dot{Q}_{w,htf} \quad 11$$

Where the subscripts "v" and "l" refer to vapour and liquid refrigerant, respectively. The heat exchanged between the refrigerant and the heat transfer fluid is given by:

$$\dot{Q}_{w,htf} = (UA)_{HEX} \cdot \left(T_{htf} - T_w\right) \quad 12$$

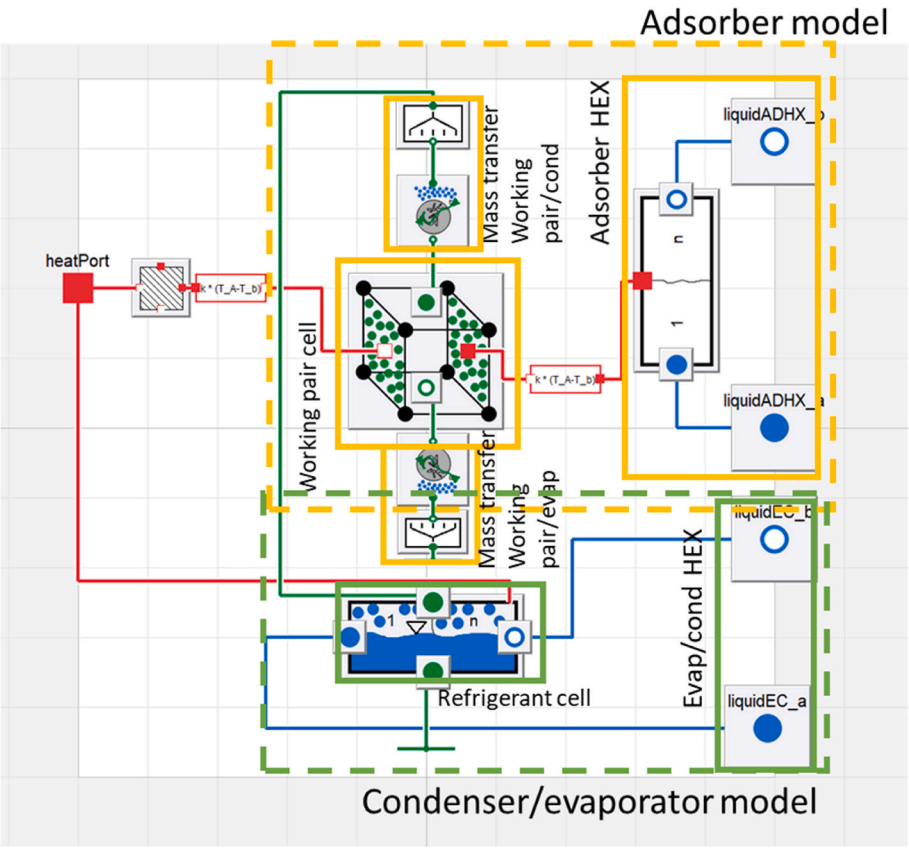

Fig. 12. Dymola layout of the model for the combined module of the chiller presented in this paper.

The model for the entire chiller consists of the model of two process modules and the corresponding boundaries for inlet/outlet of the heat transfer fluid in the three circuits (HT, MT, LT).

4.2. Model validation

In order for the optimized control logic to be actually effective, it is important that the model can represent the operation of the chiller in a wide range of conditions. Therefore, it was decided to compare it with different experimental tests, that include different cycle time, temperature and flow rates.

The deviation between the experimental and simulated results for the various cases are reported in Table 4. The column called "LT power" presents the experimentally measured cooling power, the column "LT power sim" presents the cooling power from the simulations, the column "deviation LT power" is the difference between the experimental and the simulated power, which corresponds to the error of the simulation compared to the experimental results. It is possible to notice that the deviation of the cooling power is always lower than 140 W, i.e. less than the experimental error. The same can be noticed for the COP, thus indicating that the model is able to reproduce realistically the behaviour of the prototype.

The calibrated model was exported as FMU (Functional Mock-Up Unit) [25], which includes the following inputs and outputs.

- Inputs: HT_in, MT_in, LT_in, mass flow rate HT, mass flow rate MT, mass flow rate LT, cycle time
- Outputs: power in HT circuit, power in MT circuit, power in LT circuit.

Exporting the model as FMU allows its usage for co-simulation in Python, which is used in the first step of control development.

5. Development of control logic

5.1. Meta-heuristic technique

The results from the tests carried out and described in the previous section, highlight the importance in the selection of a suitable control logic for the adsorption chiller, since it is possible to notice that there is a strong inter-dependence between various parameters (e.g. operating temperatures, flow rates and cycle time), as already discussed by some of the authors in Ref. [1]. As discussed in the introduction, the objective of the current study is to find an alternative to non-linear model predictive control frameworks, by using a meta-heuristic optimization technique.

In the vast landscape of optimization, metaheuristics represents a

Table 4
Calibration of the model.

HTin	*MTin*	*LTin*	*HT flow*	*MT flow*	*LT flow*	*LT power*	*COP*	*cycle time*	*LT power sim*	*COP sim*	*deviation LT power*	*deviation COP*
°C	°C	°C	kg/s	kg/s	kg/s	kW	–	s	kW	–	**kW**	-
68	28	17	0.9	1.2	1.03	5.9	0.53	250–400	5.9	0.53	**0.01**	**0.00**
68	28	17	0.9	1.2	0.85	5.8	0.59	250–400	5.7	0.51	**0.14**	**0.07**
68	27	17	0.9	1.2	0.56	5.4	0.56	250–400	5.3	0.49	**0.07**	**0.07**
68	27	17	0.9	1.2	0.25	4.2	0.46	250–400	4.1	0.41	**0.11**	**0.05**

powerful tool designed to tackle complex problems. These algorithms operate at a higher level, aiming to find, generate, fine-tune, or select heuristics (partial search algorithms) that yield sufficiently good solutions. They come to the rescue when information is sparse, computation capacity is limited, or the problem defies straightforward analytical approaches. The main reason for selecting meta-heuristic algorithms in the current application is linked to the strong interdependency among the different variables of the process. In terms of regions of the solution space, this means that the problem might have different solutions with completely different combination of parameters. Since meta-heuristic algorithms diversify the search in the solution space, relying on stochastic processes [26,27]. This means that the algorithms accept, as output, near-optimal solutions instead of local optima, which can lead to computational problems in complex systems with dispersed optimal combination of parameters.

For the use in the optimization of the adsorption chiller operation, the Nelder-Mead Simplex algorithm was used [28,29]. The Nelder-Mead Simplex algorithm, proposed by John Nelder and Roger Mead in 1965, belongs to the family of direct search methods. Unlike gradient-based approaches, it does not rely on derivatives or gradients of the objective function. Instead, it constructs a simplex (a geometric shape) in the parameter space and iteratively refines it to find the optimal solution, which allows its use also for objective functions whose derivative are not known or cannot be calculated. A simplex is a convex polytope formed by a set of n+1 vertices (n-dimensional points). In the context of optimization, the simplex represents a feasible region in the parameter space. The algorithm explores the search space by reflecting, expanding, or contracting the simplex.

The algorithm consists of the steps shown in Fig. 13.

5.2. Generation of synthetic data

In order for proper application of the optimization algorithm, it is necessary to generate a vast pool of data. To this aim, a Python script was realized, that calls the FMU using a wide range of inputs and their combinations,. The range of variables investigated is listed in Table 5.

Each simulation was run for 10000 s, with steps of 1 s. It is worth noticing that, for each chiller, this step only needs to be performed once, and not at each iteration of the controller, which is instead the case for the model-predictive control methods.

As subsequent step, a linear regression was carried out on the HT, MT and LT power, as a function of the three inlet temperatures, the three flow rates and the cycle time. The score for the results of the regression is shown in Fig. 14, where the relative deviation between the fitted and simulated values are compared. It is possible to notice that it lies between −0.75 and + 1.00, thus indicating a good fitting.

The fitted expressions for the three powers are reported in Appendix.

5.3. Optimization of settings

Once the generated data were available, the fitting expressions were used for the optimization steps. Two possible objective functions were defined and used for the Nelder-Meal Simplex Algorithm: maximization of the cooling power and maximization of the COP. The variables whose values have to be calculated are the flow rates and the cycle time. The following boundaries were specified, which are wider than the experimental conditions tested.

- Flow rates limited between 0.5 and 5 kg/s
- Cycle time between 600 s and 2500 s.

The optimization results are displayed as a sort of performance table, that can be easily implemented in the PLC of the chiller. An example for some operating conditions and optimization of the cooling power is shown in Table 6.

Table 5
List of conditions for the generation of synthetic data.

Variable	Unit	Initial value	Final Value	delta_value
HT_in	°C	65	90	5
MT_in	°C	20	40	5
LT_in	°C	12	20	2
flow rate HT	kg/s	0.5	1.5	0.25
flow rate MT	kg/s	1.5	3	0.5
flow rate MT	kg/s	0.5	1.5	0.25
cycle_time	s	800	1800	250

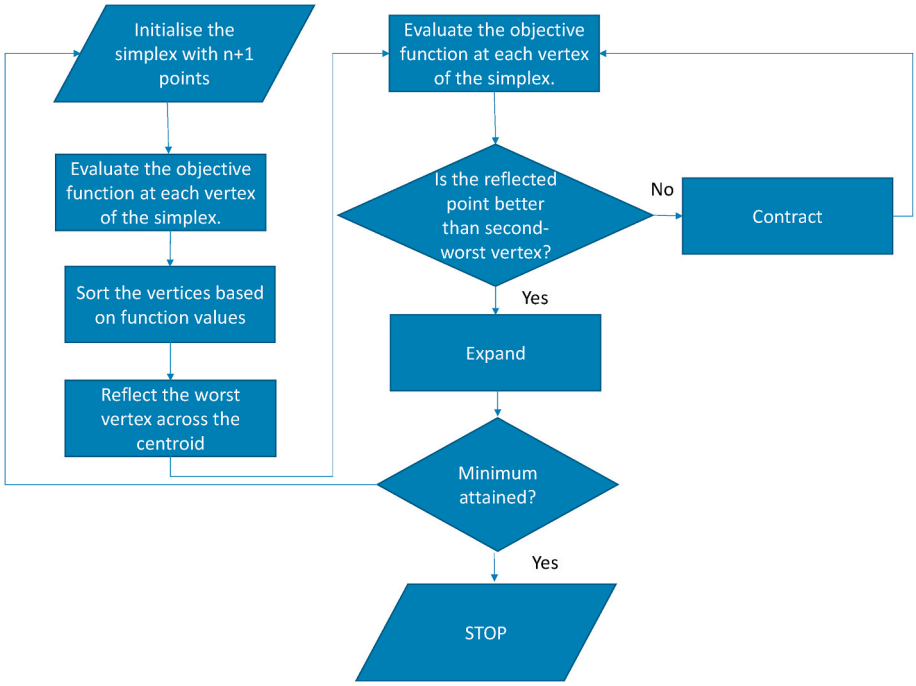

Fig. 13. Flowchart for the Nelder-Mead algorithm.

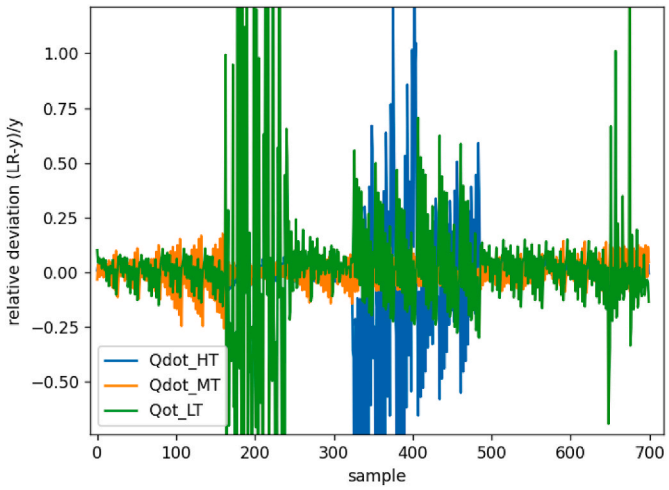

Fig. 14. Score of linear fitting for the three powers.

6. Experimental verification of optimized control logic

After the optimization procedure was completed, its effectiveness was assessed by repeating some testing conditions with the optimal set parameters for cycle time and flow rates. In this testing step, the cycle time was set as fixed, thus not allowing the internal control of the chiller to vary it.

The results are reported in Table 7: the different test sets are reported and separated by larger lines; the test with blue background are the reference ones (i.e. those carried out without any optimized setting). For the other tests, the variation of the cooling power and COP with respect to the benchmarking test is reported. Since in some temperature conditions the optimal sets for maximizing the cooling power and maximizing the COP were different, the tests with orange background are specifically intended to verify the improvement of the COP.

It is possible to notice that, for all testing conditions, there is always an improvement of the performance in the verification tests compared to the original conditions. Such improvement, for the cooling power, is in the range of 6 %–31 %; For the testing conditions intended to maximise the COP, there is always an improvement, from 3 % to 11 %. It is worth mentioning that a single objective function was used for the present study, i.e. maximizing cooling power or maximizing COP. It might be possible to use an objective function which corresponds to simultaneous increase of both cooling power and COP, but this would somehow result in a trade-off between the two values. As described in several literature works, increasing COP often results in a reduction of cooling power and viceversa. As an example, Bau et al. used a non-linear model predictive control strategy and showed the Pareto frontier for the specific cooling power- COP case [30]. Similarly to the results obtained in the current tests, either a trade-off solution is sought, or the maximization of a single objective can be achieved: for the maximum COP, the specific cooling power might be lower than the reference one and for the maximum cooling power, the achievable COP will be lower than the reference case.

7. Considerations on the implementation in the PLC

The proposed method can be easily implemented in an industrial PLC, as the one with which the tested prototype is equipped, in the form of a map of settings as a function of the three operating temperatures (HT, MT, LT). The flowchart for the implementation is presented in Fig. 15. It is possible to notice that the operations to be performed are simple and, for each chiller, the calibration of the dynamic model can be done by the manufacturer based on 5 to 10 experimental points, thus making the proposed methodology easily and widely applicable also in industrial environment. Therefore, it is possible to state that the novelty of our method lies in its simplicity and deployability: the proposed control system synthesizes optimal operating conditions into a lookup table that can be implemented on standard programmable logic controllers, eliminating the need for high-performance industrial PCs or complex real-time computations. This ensures scalability to industrial applications, where ease of integration, reliability, and cost-effectiveness are critical. The final outcome of the research carried out is a simple and yet effective way to improve the energy efficiency of adsorption chillers, in terms of COP and cooling power, without modifications to system components.

8. Conclusions and future perspectives

The present paper presented a methodological framework for the realization and implementation of a control strategy for adsorption chillers. To this aim, a small-scale prototype with 6 kW nominal cooling power was tested. The experimental results were used to validate a dynamic model of the chiller realized in Modelica/Dymola, which was exported as FMU and used to generate up to 32000 points of synthetic data. Using the Nelder-mead simplex algorithm, the synthetic data were processed and a “settings map” was generated, which includes the optimal cycle time and flow rates of heat transfer fluid circuits according to the operating temperatures of the chiller. Two different objective functions were tested, i.e. to maximise the cooling power or to maximise the COP. Dedicated tests were carried out with the optimal parameters and the results highlighted that, for all testing conditions, there is always an improvement of the performance in the verification tests compared to

Table 6
Example of the optimization output with maximization of cooling power as objective function.

condition ID	HT	MT	LT	cooling power	HT flow	MT flow	LT flow	cycle time
–	K	K	K	kW	kg/s	kg/s	kg/s	s
1	338.15	298.15	287.15	0.59	0.95	2.07	0.99	2000
2	338.15	298.15	289.15	0.64	0.95	2.06	0.86	2000
3	338.15	298.15	291.15	0.69	0.95	2.05	1.10	2000
7	338.15	303.15	291.15	0.64	0.95	2.06	1.04	1300
8	338.15	308.15	285.15	0.08	0.95	2.15	1.56	800
10	338.15	308.15	289.15	0.18	0.95	2.13	1.20	1200
11	338.15	308.15	291.15	0.52	0.95	2.08	1.42	2000
22	343.15	303.15	289.15	0.49	0.95	2.09	1.57	2000
23	343.15	303.15	291.15	0.57	0.95	2.08	0.97	1500
24	343.15	308.15	285.15	0.10	0.95	2.15	0.93	800
25	343.15	308.15	287.15	0.15	0.95	2.14	1.36	800
26	343.15	308.15	289.15	0.25	0.95	2.13	1.29	2000
27	343.15	308.15	291.15	0.42	0.95	2.10	1.48	2000
31	343.15	313.15	291.15	0.12	0.95	2.14	1.03	800
32	348.15	298.15	285.15	0.43	0.95	2.10	0.95	1000
33	348.15	298.15	287.15	0.50	0.95	2.09	0.95	1100

Table 7
Experimental verification of improved performance.

ID	HTin	MTin	LTin	LTout	V_HT	V_MT	V_LT	Q_LT	COP	cycle time	ΔQ_LT	Δ_COP
	K	K	K	K	kg/s	kg/s	kg/s	kW	–	s	%	%
8	74.18	28.56	15.30	14.05	0.92	1.18	1.03	4.21	0.55		-	-
42	*74.03*	*29.47*	*11.71*	*11.25*	*0.92*	*1.83*	*1.13*	*2.61*	*0.57*	*2000*	***62 %***	***103 %***
44	*73.38*	*25.46*	*10.45*	*9.78*	*0.92*	*1.83*	*1.13*	*3.42*	*0.58*	*1800*	***81 %***	***105 %***
6	72.59	31.21	18.06	15.99	0.91	1.16	1.02	5.17	0.52	–	-	-
39	71.66	32.07	18.66	17.64	0.73	1.83	1.14	5.47	0.59	1000	**106 %**	**113 %**
33	67.70	25.02	14.77	13.00	0.92	1.67	0.84	6.68	0.55	–	-	-
36	66.71	25.48	14.63	13.42	0.73	1.67	1.10	7.76	0.62	600	**116 %**	**114 %**
26	68.18	27.77	16.53	15.03	0.91	1.19	0.85	5.84	0.59	250–400	-	-
37	69.43	26.28	16.77	15.23	0.73	1.83	1.14	7.62	0.62	800	**131 %**	**105 %**
40	69.45	26.11	17.93	16.64	0.73	1.83	1.14	6.46	0.48	800	**111 %**	**82 %**
11	72.03	29.00	18.16	16.72	0.91	1.19	1.03	6.59	0.60	–	-	-
38	71.06	29.49	17.88	16.59	0.73	1.83	1.14	6.68	0.62	1000	**102 %**	**104 %**
19	61.47	24.95	13.23	12.19	0.92	1.18	1.03	4.91	0.56	–	-	-
41	61.35	25.69	14.10	13.09	0.73	1.83	1.13	5.29	0.53	800	**108 %**	**94 %**
15	*73.14*	*27.58*	*13.24*	*12.21*	*0.92*	*1.18*	*1.02*	*4.80*	*0.60*	-	-	-
43	*73.78*	*27.00*	*13.27*	*12.63*	*0.92*	*1.83*	*1.13*	*3.34*	*0.62*	*1700*	***69 %***	***104 %***
45	*73.41*	*26.50*	*13.36*	*12.49*	*0.92*	*1.83*	*1.13*	*4.28*	*0.65*	*1600*	***89 %***	***108 %***

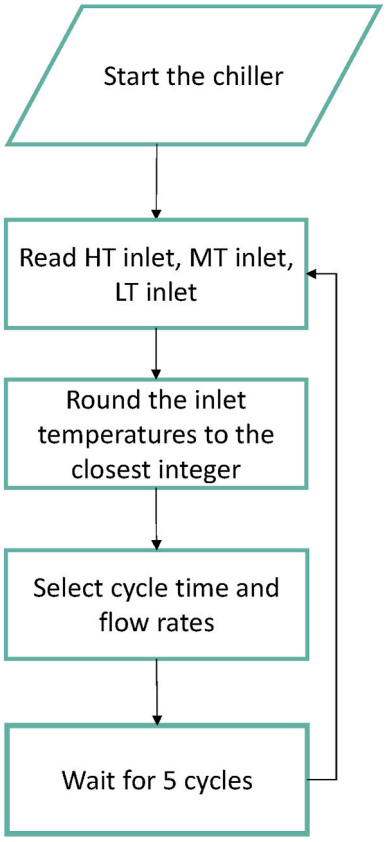

Fig. 15. Flowchart for the implementation of the proposed control strategy in a PLC.

the original conditions. Such improvement, for the cooling power, is in the range of 6 %–31 % and, for the COP, is in the range 3 %–11 %. Finally, the flowchart which described the implementation of the tested strategy into an industrial PLC was generated, which highlights the effective potential for the application in industrial context, even using low-end PLCs. The approach followed in the current research is intended to ensure industrial applicability, as many facilities prioritize simple, robust solutions over complex, high-maintenance alternatives. Starting from this outcomes, future works can focus on long-term energy performance analysis, comparing COP and cooling capacity against conventional control methods in real-world settings, Integration with hybrid systems, such as solar-thermal or waste-heat recovery networks, to assess the controller's adaptability to fluctuating heat sources and edge-computing enhancements, exploring how low-cost IoT devices could enable adaptive updates to the lookup table while retaining PLC compatibility.

CRediT authorship contribution statement

Valeria Palomba: Writing – original draft, Project administration, Methodology, Investigation, Funding acquisition, Formal analysis, Data curation, Conceptualization. **Antonino Bonanno:** Validation, Investigation, Formal analysis, Data curation. **Giovanni Brunaccini:** Validation, Software, Methodology, Investigation, Conceptualization. **Fabio Costa:** Investigation. **Davide La Rosa:** Investigation. **Andrea Frazzica:** Writing – review & editing, Visualization, Validation, Methodology, Conceptualization.

Declaration of competing interest

The authors declare that they have no known competing financial interests or personal relationships that could have appeared to influence the work reported in this paper.

Acknowledgments

The present work is funded by the European Commission under the H2020 Framework under Grant Agreement 955413 (ENGIMMONIA).

Appendix A

The fitted expressions for the three powers are reported in Table 8. The cycle time is in s, all the temperatures in K, and the flow rates in kg/s.

Table 8
fitted expressions for the powers

HT	qHT [W] = 137750.5148 + 0.0 * HT^1 -0.0 * HT^2 + 0.0025 * HT^3 -0.0134 * MT^1–4.059 * MT^2 + 0.0033 * MT^3 + 0.0 * LT^1 + 0.0 * LT^2 + 0.0026 * LT^3 + 1739.3816 * Hm^1–425.9551 * Hm^2 + 2132.2755 * Mm^1–224.4237 * Mm^2 + 1316.4305 * Lm^1–291.0942 * Lm^2 + 0.0 * ct^1 + 0.0106 * ct^2 -0.0 * ct^3
MT	qMT [W] = −43862.1204 -0.0 * HT^1 -0.0 * HT^2 -0.0007 * HT^3 + 0.0028 * MT^1 + 0.8606 * MT^2 -0.0024 * MT^3 + 0.0 * LT^1 + 0.0 * LT^2 + 0.0014 * LT^3 + 1390.1841 * Hm^1–316.3239 * Hm^2 + 2265.295 * Mm^1–139.8413 * Mm^2 + 272.4974 * Lm^1 + 177.3098 * Lm^2 -0.0 * ct^1 -0.0096 * ct^2 + 0.0 * ct^3
LT	qLT [W] = −96184.283 -0.0 * HT^1 + 0.0 * HT^2 -0.0012 * HT^3 + 0.0112 * MT^1 + 3.3795 * MT^2 -0.0015 * MT^3 -0.0 * LT^1 -0.0 * LT^2 -0.0048 * LT^3–3881.5077 * Hm^1 + 870.8775 * Hm^2–2856.6433 * Mm^1 + 248.2025 * Mm^2–3159.9804 * Lm^1 + 353.6579 * Lm^2 -0.0 * ct^1 -0.0015 * ct^2 -0.0 * ct^3

Data availability

Data will be made available on request.

References

[1] Palomba V, Dino GE, Frazzica A. Coupling sorption and compression chillers in hybrid Cascade layout for efficient exploitation of renewables: sizing, design and optimization. Renew Energy 2020;154:11–28. https://doi.org/10.1016/j.renene.2020.02.113.

[2] Shmroukh AN, Ali AHH, Ookawara S. Adsorption working pairs for adsorption cooling chillers: a review based on adsorption capacity and environmental impact. Renew Sustain Energy Rev 2015;50:445–56. https://doi.org/10.1016/j.rser.2015.05.035.

[3] Palomba V, Vasta S, Giacoppo G, Calabrese L, Gulli G, La Rosa D, et al. Design of an innovative graphite exchanger for adsorption heat pumps and chillers. Energy Proc 2015;81:1030–40. https://doi.org/10.1016/j.egypro.2015.12.112.

[4] Grekova A, Tokarev M. An optimal plate fin heat exchanger for adsorption chilling: theoretical consideration. International Journal of Thermofluids 2022;16:100221. https://doi.org/10.1016/j.ijft.2022.100221.

[5] Mikhaeil M, Gaderer M, Dawoud B. On the development of an innovative adsorber plate heat exchanger for adsorption heat transformation processes; an experimental and numerical study. Energy 2020;207:118272. https://doi.org/10.1016/j.energy.2020.118272.

[6] Gibelhaus A, Tangkrachang T, Bau U, Seiler J, Bardow A. Integrated design and control of full sorption chiller systems. Energy 2019;185:409–22. https://doi.org/10.1016/j.energy.2019.06.169.

[7] Sapienza A, Palomba V, Gullì G, Frazzica A, Vasta S. A new management strategy based on the reallocation of ads-/desorption times: experimental operation of a full-scale 3 beds adsorption chiller. Appl Energy 2017;205:1081–90. https://doi.org/10.1016/j.apenergy.2017.08.036.

[8] Chorowski M, Pyrka P, Rogala Z, Czupryński P. Experimental study of performance improvement of 3-Bed and 2-Evaporator adsorption chiller by control optimization. Energies 2019;12:3943. https://doi.org/10.3390/en12203943.

[9] Krzywanski J, Skrobek D, Sosnowski M, Ashraf WM, Grabowska K, Zylka A, et al. Towards enhanced heat and mass exchange in adsorption systems: the role of AutoML and fluidized bed innovations. Int Commun Heat Mass Tran 2024;152:107262. https://doi.org/10.1016/j.icheatmasstransfer.2024.107262.

[10] Kalawa W, Sztekler K, Mlonka-Mędrala A, Radomska E, Nowak W, Mika Ł, et al. Simulation analysis of mechanical fluidized bed in adsorption chillers. Energies 2023;16:5817. https://doi.org/10.3390/en16155817.

[11] Albers J. Enhanced characteristic equation method for single-stage absorption heat pumps. Int J Refrig 2025;169:124–39. https://doi.org/10.1016/j.ijrefrig.2024.09.028.

[12] Bau U, Bardow A. Pareto-optimal performance of one-bed adsorption chillers by easy-to-implement heat-flow-based control. Appl Therm Eng 2019;159:113590. https://doi.org/10.1016/j.applthermaleng.2019.03.161.

[13] Krzywanski J, Grabowska K, Herman F, Pyrka P, Sosnowski M, Prauzner T, et al. Optimization of a three-bed adsorption chiller by genetic algorithms and neural networks. Energy Convers Manag 2017;153:313–22. https://doi.org/10.1016/j.enconman.2017.09.069.

[14] Krzywanski J, Skrobek D, Zylka A, Grabowska K, Kulakowska A, Sosnowski M, et al. Heat and mass transfer prediction in fluidized beds of cooling and desalination systems by AI approach. Appl Therm Eng 2023;225:120200. https://doi.org/10.1016/j.applthermaleng.2023.120200.

[15] Panahizadeh F, Hamzehei M, Farzaneh-Gord M, Villa AAO. Evaluation of machine learning-based applications in forecasting the performance of single effect absorption chiller network. Therm Sci Eng Prog 2021;26:101087. https://doi.org/10.1016/j.tsep.2021.101087.

[16] Hong G, Seong N. Optimization of the ANN model for energy consumption prediction of direct-fired absorption chillers for a short-term. Buildings 2023;13:2526. https://doi.org/10.3390/buildings13102526.

[17] Kim J-H, Seong N-C, Choi W. Forecasting the energy consumption of an actual air handling unit and absorption chiller using ANN models. Energies 2020;13:4361. https://doi.org/10.3390/en13174361.

[18] Lazrak A, Boudehenn F, Bonnot S, Fraisse G, Leconte A, Papillon P, et al. Development of a dynamic artificial neural network model of an absorption chiller and its experimental validation. Renew Energy 2016;86:1009–22. https://doi.org/10.1016/j.renene.2015.09.023.

[19] K L, K S, B M, S J, L M, M A, et al. From detection to action: implementing deep learning inference in PLC systems via docker services. IFAC-PapersOnLine 2024;58:19–24. https://doi.org/10.1016/j.ifacol.2024.07.365.

[20] Al-Hasni S, Santori G. The cost of manufacturing adsorption chillers. Therm Sci Eng Prog 2023;39:101685. https://doi.org/10.1016/j.tsep.2023.101685.

[21] Velte-Schäfer A, Zhang Y, Nonnen T, Wittstadt U, Frazzica A, Füldner G, et al. Numerical modelling and evaluation of a novel sorption module for thermally driven heat pumps and chillers using open-source simulation library. Energy Convers Manag 2023;291:117252. https://doi.org/10.1016/j.enconman.2023.117252.

[22] Palomba V, Bonanno A, Brancato V, Frazzica A, Herrmann R. Design of adsorption chillers under rolling conditions in naval applications: experimental and numerical approaches. Appl Therm Eng 2024;248:123224. https://doi.org/10.1016/j.applthermaleng.2024.123224.

[23] Brancato V, Frazzica A. Characterisation and comparative analysis of zeotype water adsorbents for heat transformation applications. Sol Energy Mater Sol Cell 2018;180:91–102. https://doi.org/10.1016/j.solmat.2018.02.035.

[24] Zhang Y, Palomba V, Frazzica A. Understanding the effect of materials, design criteria and operational parameters on the adsorption desalination performance – a review. Energy Convers Manag 2022;269:116072. https://doi.org/10.1016/j.enconman.2022.116072.

[25] Functional Mock-up interface n.d. https://fmi-standard.org/(accessed February 12, 2025).

[26] Nassef AM, Abdelkareem MA, Maghrabie HM, Baroutaji A. Review of metaheuristic optimization algorithms for power systems problems. Sustainability 2023;15:9434. https://doi.org/10.3390/su15129434.

[27] Ezugwu AE, Shukla AK, Nath R, Akinyelu AA, Agushaka JO, Chiroma H, et al. Metaheuristics: a comprehensive overview and classification along with bibliometric analysis. Artif Intell Rev 2021;54:4237–316. https://doi.org/10.1007/s10462-020-09952-0.

[28] Fakhouri HN, Hudaib A, Sleit A. Hybrid particle swarm optimization with sine cosine algorithm and nelder–mead simplex for solving engineering design problems. Arabian J Sci Eng 2020;45:3091–109. https://doi.org/10.1007/s13369-019-04285-9.

[29] Pedroso JP. Simple metaheuristics using the simplex algorithm for non-linear programming. In: Stützle T, Birattari M, H. Hoos H, editors. Engineering stochastic local search algorithms. Designing, implementing and analyzing effective heuristics, vol. 4638. Berlin, Heidelberg: Springer Berlin Heidelberg; 2007. p. 217–21. https://doi.org/10.1007/978-3-540-74446-7_21.

[30] Bau U, Baumgärtner N, Seiler J, Lanzerath F, Kirches C, Bardow A. Optimal operation of adsorption chillers: first implementation and experimental evaluation of a nonlinear model-predictive-control strategy. Appl Therm Eng 2019;149:1503–21. https://doi.org/10.1016/j.applthermaleng.2018.07.078.